Numerical Modelling Study of the 2016 Gyeongju Earthquake Rupture Process and Correlation with Groundwater Level Change

Jeoung Seok Yoon
DynaFrax UG (haftungsbeschränkt), Potsdam, Germany

Anne Strader
DynaFrax UG (haftungsbeschränkt), Potsdam, Germany

Jian Zhou
Beijing University of Technology, Beijing, China

Soo-Gin Kim
Korea Radioactive Waste Agency, Gyeongju, Korea

Jae-Yeol Cheong
Korea Radioactive Waste Agency, Gyeongju, Korea

ABSTRACT: Coseismic changes in groundwater level have been reported worldwide, particularly in areas of moderate to high seismicity. These variations are often attributed to redistribution of stress and strain, which can reactivate fractures, joints and microcracks through local changes in fluid pressure. Such variations were observed following the September 2016 ML 5.8 Gyeongju earthquake in South Korea, rupturing the Yangsan fault at a depth of 11–16 km and producing strong high-frequency ground motions. To better understand and quantify local stress changes and subsequent changes in fluid migration patterns within this area, we have developed a discrete element model (DEM) of the Yangsan fault network using the Particle Flow Code (PFC2D) software. Spatial distributions of local Coulomb stress changes are in good agreement with stress changes reported in literature. Furthermore, a weak but positive correlation is observed between the amount of groundwater level change and increased stress.

Keywords: Discrete element model, numerical modeling, rupture simulation, Korean seismicity, fluid migration.

1 INTRODUCTION

Coseismic changes in groundwater level have been observed in many seismically active places of the world (Chia et al. 2008 and Shi et al. 2015). When seismic waves pass through a well, the seismic shaking of the water column and its connected aquifer results in an oscillatory change in water level. In the vicinity of earthquake epicenters, abrupt step-like groundwater level changes have been recorded during earthquakes. Such variations usually are sustained from a few days to several months, and thus can be identified immediately after strong earthquakes. In the case of the MW 7.9 Wenchuan earthquake in China, Shi et al. (2015) hypothesized that as the volumetric strain decreases (contraction), groundwater level should increase, and vice versa in the case of increased volumetric strain (tension).

On September 2016, the ML 5.1 and ML 5.8 Gyeongju earthquakes ruptured a subsurface strike-slip branch of the Yangsan fault in southeast Korea at a depth of 11–16 km and an approximate length of 26 km, striking N27°E with a dip of 65° to the east. The earthquake triggered a series of more than

500 aftershocks, producing strong high-frequency ground motions and causing extensive damage throughout the region. These earthquakes caused coseismic changes in both static and dynamic stress, which have been hypothesized in numerous previous studies to alter medium properties such as permeability, resulting hydrologic and hydrogeologic changes including changes in groundwater levels (Lee et al. 2021a; Lee et al. 2021b; Kim et al. 2018). Figure 1 (Figure 1 from Kim et al. 2018) displays the locations of the Gyeongju earthquake epicenters as well as the monitoring well locations near the earthquakes, many of which recorded coseismic groundwater changes following the earthquakes (Figure 2; Figure 2 from Kim et al. 2018).

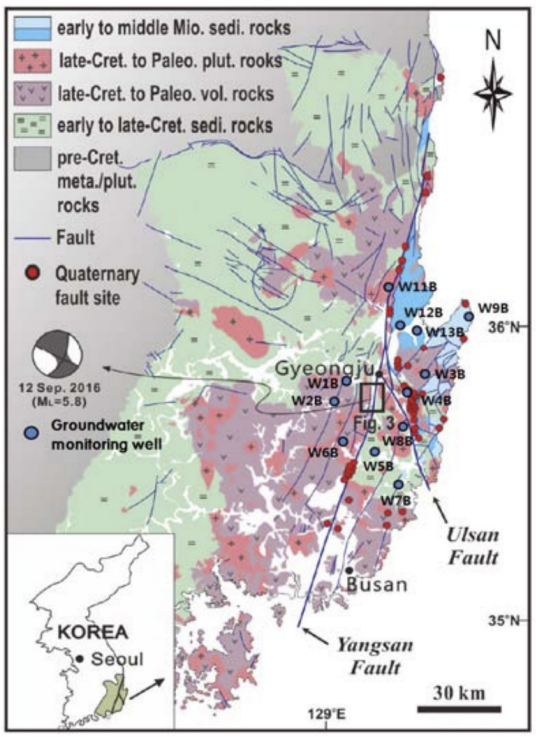

Figure 1. Figure 1 from Kim et al. (2018). Geologic map of the Korean study region, showing the location of groundwater monitoring wells.

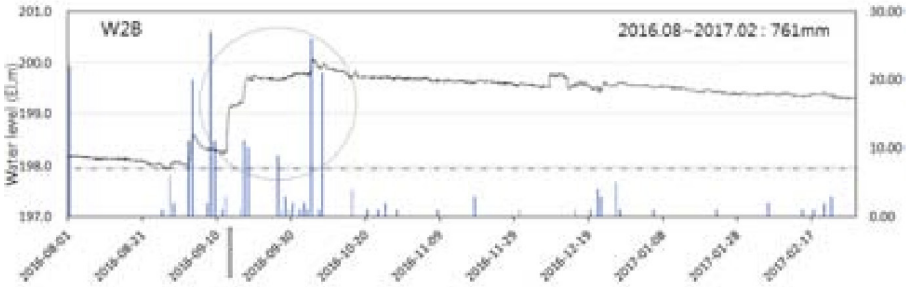

Figure 2. Figure 2b from Kim et al. (2018). Time series of groundwater levels and rainfall at well W2B (see Figure 1), displaying the time of the 2016 Gyeongju earthquake (vertical line on x-axis). A sharp, step-like increase in groundwater level is observed following the mainshock.

2 METHODS

We generated a 2D discrete element geological model of the south-east region of Korea using Itasca's Particle Flow Code (PFC2D) (Figure 3b). The rock mass is represented by a bonded particle assembly, where the circular particles are bonded at their contacts by the soft bond model. We used

a CAD-based fault structure model (Figure 3a), consisting of 43 faults, representing the contacts at faults using the smooth joint contact model (Mas Ivars et al. 2011). Table 1 lists the physical parameters of the smooth joints. The study area domain was 120 km x 180 km, and the particle radii ranged from 200–300 m, with 93318 particles in total, considering model convergence when applying in-situ stress, avoiding excessive computation times, and consistency with local geology.

Table 1. Physical properties of modeled faults (smooth joint model). All parameter values were best estimates, based on study region lithology and combinations of properties that resulted in model stability.

Parameter		Value
Contact model type	[-]	Smooth joint
Normal stiffness/area	[Pa/m]	300e6
Shear stiffness/area	[Pa/m]	50e6
Friction coefficient	[-]	0.6
Cohesion	[Pa]	5e6
Tensile strength	[Pa]	1e6
Joint friction angle	[°]	30
Dilation angle	[°]	3
Joint bond state	[-]	bonded

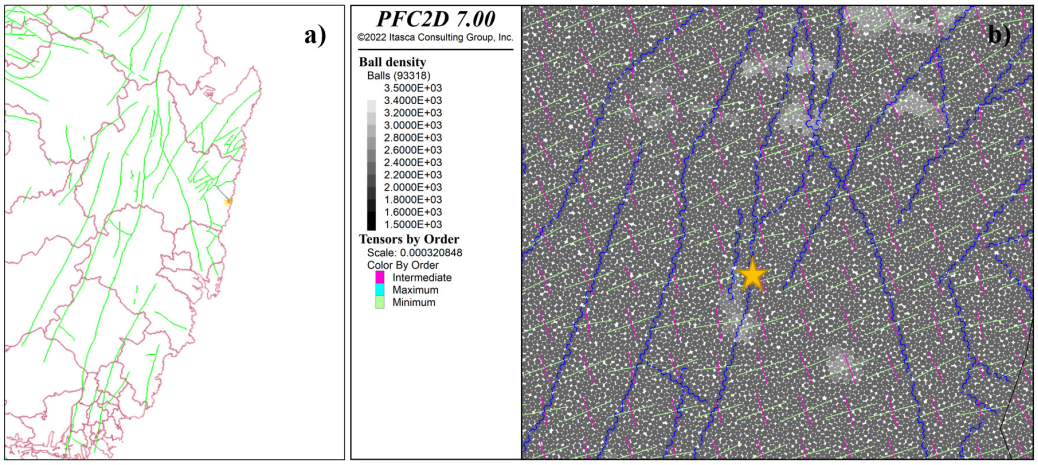

Figure 3. a) CAD-based fault structure model of south-east Korea. b) Closeup image of PFC2D geological model of south-east Korea. The blue lines represent fault locations, represented by smooth joints, and the location of the mainshock is indicated by the yellow star. Grayscale variations show spatial variations in particle density (Choi et al. 2022). Principal stress component orientations are displayed throughout the study region; here, minimum principal stress corresponds to maximum compression.

After initialization of the domain and particle assembly, a parallel-bonded sample was created using the soft bond contact model. The modeled density was based on spatial variations throughout the study region derived from gravity variations (Choi et al. 2022; see density variations of particles in Figure 3b). The faults along with their respective physical properties were then inserted into the model.

To simulate the dynamic rupture process, we used the “lock and release” approach by Yoon et al. (2017). In this approach, a finite length of the fault at the hypocenter location was locked during in-situ stress initialization (maximum and minimum compressive horizontal stresses of 16.85 MPa and 10.8 MPa, respectively) in order to accumulate strain energy. After reaching in-situ stress levels, the stored strain energy was released by unlocking the locked part of the fault. The in-situ stress components were calculated from a linear scaling relation expressing principal stress magnitudes of functions of depth; Figure 4 shows the relations between maximum and minimum horizontal stresses with depth, respectively. A locking radius of 1400 m, corresponding to a fault length of 2800 m, was

applied. The fault geometry was calibrated based on fault scaling relations introduced by Wells and Coppersmith (1994), to result in an event moment magnitude consistent with that of the mainshock.

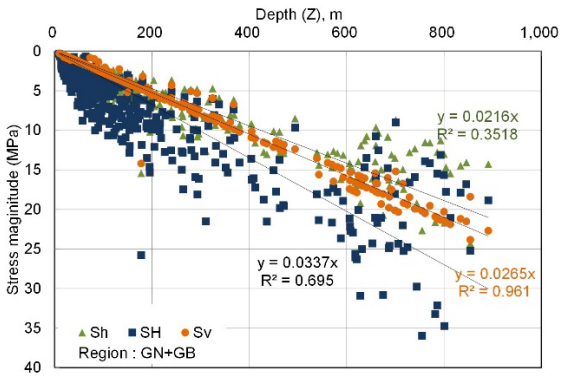

Figure 4. Linear scaling relation between principal stress magnitudes and depth, representative for south-east Korea.

3 RESULTS

3.1 Dynamic rupture simulation

The simulated rupture propagation is displayed in Figure 5 at 1 s, 5 s, 10 s and 30 s after the start of the modeled rupture process. The particle colors show their velocities at the given timesteps, while the smooth joint contact colors (representing fault locations) display the amount of slip. Overall, the wave propagation appears consistent to those of recorded seismic events.

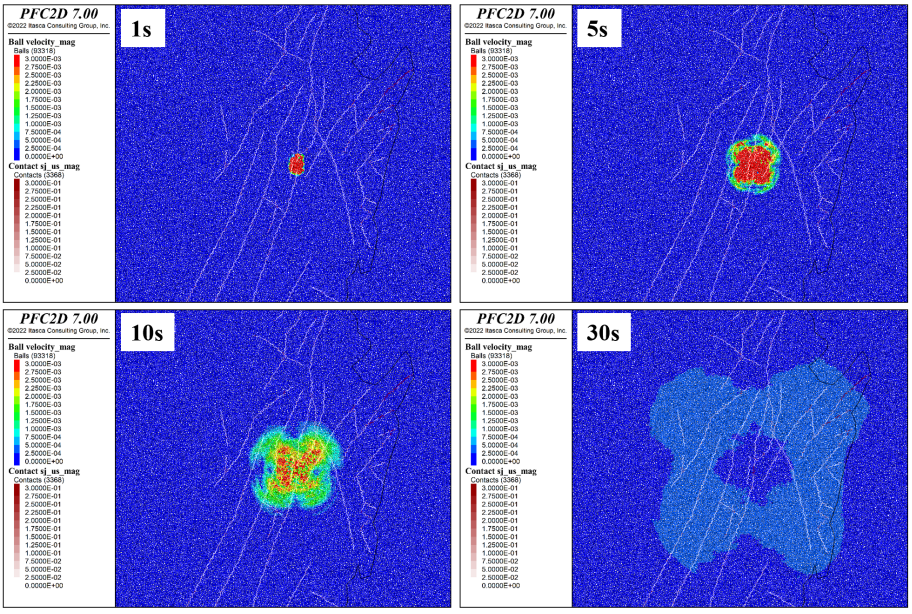

Figure 5. Propagation of the simulated seismic wave. The particle colors represent ball velocity magnitudes (m/s), while the fault colors show the amount of slip (m).

The maximum amount of slip that occurred along the modeled Yangsan fault during the simulation was just over 0.8 m. The slip distribution showed a tapered pattern, consistent with observed earthquake slip distributions. The amount of simulated slip was also consistent with a ML 5.8 (corresponding to MW 5.4) strike-slip earthquake along a fault length of 2800 m. Zoback and

Gorelick (2012) present an empirical scaling relation between fault length, slip amount, magnitude and stress drop, upon which we evaluated the ability of PFC2D to accurately replicate the Gyeongju earthquake rupture process.

3.2 Coseismic groundwater level changes and stress changes

Using the method from Okada (1992), we calculated coseismic Coulomb stress changes based on the slip distribution, in order to evaluate the consistency between stress changes based on the PFC2D simulation and on the observed Gyeongju earthquake slip distribution. Before calculating the changes in the three-dimensional stress tensor, the fault geometry model was extended from 2D to 3D through the application of fault scaling relations introduced by Wells and Coppersmith (1994). Following the calculation of stress tensor component changes, Coulomb stress changes were determined by resolving the stress tensor changes onto a uniform, right-lateral, vertical receiver plane orientation with a strike angle of 115°. Figure 6a displays Coulomb stress changes from the simulated slip distribution. Overall, the spatial distribution of Coulomb stress changes is in good agreement with those reported in previous studies such as Hong et al. (2017), indicating that PFC2D is capable of producing slip distributions that yield coseismic stress changes similar to those derived from observed slip.

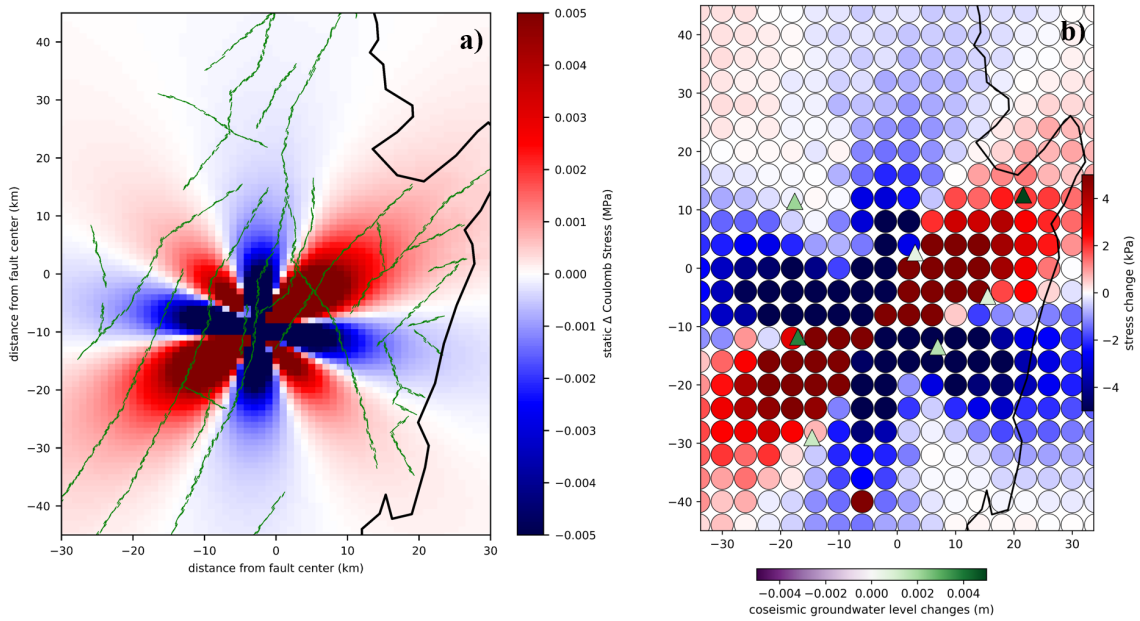

Figure 6. a) Coseismic static Coulomb stress changes, calculated from the PFC2D-modeled slip distribution. Red zones indicate where Coulomb stress has increased; blue zones where Coulomb stress has decreased. b) Static coseismic change in maximum horizontal stress. Tension is considered positive; compression is considered negative. The triangles show well locations, and their colors indicate the amount of coseismic groundwater level change recorded following the Gyeongju earthquake.

The spatial distribution of changes in maximum principal horizontal stress is displayed in Figure 6b, along with recorded coseismic groundwater level changes at well locations. Coseismic increases in groundwater level were recorded in nearly all wells, including those outside of the closeup area in Figure 6b. In areas where maximum horizontal stress decreased, indicating compression, positive groundwater elevation changes were observed, which is consistent with our original hypothesis. The same conclusions regarding correlation between Coulomb stress change and groundwater level change can be reached. However, groundwater elevation also increased in areas of tension, where maximum horizontal stress increased, suggesting that the overall correlation between stress changes and groundwater elevation may be weaker than originally hypothesized.

4 CONCLUSIONS AND DISCUSSION

Through modeling the Gyeongju earthquake rupture in PFC2D, we were able to accurately replicate the dynamic rupture process, as well as reliably quantify changes in the stress field. Groundwater levels tended to increase in areas that were compressed by the mainshock (negative stress changes). This supports the original hypothesis proposed by Shi et al. (2015). However, similar groundwater elevation changes were observed where tension occurred due to positive stress changes.

The apparent negligible difference between groundwater level changes in areas of compression and tension could be attributed to factors other than stress change, such as local lithological and tectonic variations, pre-existing fracture network density, or well elevation. Furthermore, many wells were located at distances far enough from the modeled earthquake epicenter that stress changes had decayed considerably. Shi et al. (2015) observed that following the Wenchuan earthquake, far-field coseismic changes in groundwater level were too large to be completely explained by the small stress changes at the well locations. The relative impact of local factors within the Korean study region on groundwater response therefore requires further investigation.

REFERENCES

Chia, Y., Chiu, J. J., Chian, Y.-H., Lee, T.-P., Wu, Y.-M., & Horng, M.-J. 2008. Implications of coseismic groundwater level changes observed at multiple-well monitoring stations. *Geophysical Journal International* 172, pp. 293-301.

Choi, S., Kim, S.-W., Yoon, J.-S., & Choi, E.-K. 2022. Tectonic evolution of the Yangsan Fault, SE-Korea estimated by gravity field interpretation. *In review*.

Hong, T.-K., Lee, J., Kim, W., Hahm, I.-K., Woo, N. C., & Park, S. 2017. The 12 September 2016 ML5.8 midcrustal earthquake in the Korean peninsula and its seismic implications. *Geophysical Research Letters* 44, pp. 3131-3138.

Kim, H., Synn, J.-H., Park, C., Song, W. K., Park, E. S., Jung, Y.-B., Cheon, D.-S., Bae, S., Choi, S.-O., Chang, C., & Min, K.-B. 2021. Korea stress map 2020 using hydraulic fracturing and overcoring data. *Tunnel & Underground Space* 31 (3), pp. 145-166.

Kim, G.-B., Choi, M.-R., Lee, C.-J., Shin, S.-H., & Kim, H.-J. 2018. Characteristics of spatio-temporal distribution of groundwater level's change after 2016 Gyeong-ju earthquake. *Journal of the Geological Society of Korea* 54 (1), pp. 93-105.

Lee, S.-H., Lee, J. M., Moon, S.-H., Ha, K., Kim, Y., Jeong, D. B., & Kim, Y. 2021a. Seismically induced changes in groundwater levels and temperatures following the Ml5.8 (Ml5.1) Gyeongju earthquake in South Korea. *Hydrogeology Journal* 29, pp. 1679-1689.

Lee, A. H., Hamm, S.-Y., & Woo, N. C. 2021b. Pilot-scale groundwater monitoring network for earthquake surveillance and forecasting research in Korea. *Water* 13, p. 2448.

Mas Ivars, D., Pierce, M. E., Darcel, C., Reyes-Montes, J., Potyondy, D. O., Young, R. P., & Cundall, P. A. 2011. The synthetic rock mass approach for jointed rock mass modelling. *International Journal of Rock Mechanics & Mining Sciences* 48, pp. 219-244.

Okada, Y. 1992. Internal deformation due to shear and tensile faults in a half-space. *Bulletin of the Seismological Society of America* 82, pp. 1018-1040.

Shi, Z., Wang, G., Manga, M., & Wang, C.-Y. 2015. Continental-scale water-level response to a large earthquake. *Geofluids* 15, pp. 310-320.

Wells, D. L. & Coppersmith, K. J. 1994. New empirical relationships among magnitude, rupture length, rupture width, rupture area, and surface displacement. *Bulletin of the Seismological Society of America* 84 (4), pp. 974-1002.

Yoon, J. S., Stephansson, O., Zang, A., Min, K.-B., & Lanaro, F. 2017. Discrete bonded particle modelling of fault activation near a nuclear waste repository site and comparison to static rupture earthquake scaling laws. *International Journal of Rock Mechanics & Mining Sciences* 98, pp. 1-9.

Zoback, M. D. & Gorelick, S. M. 2012. Earthquake triggering and large-scale geologic storage of carbon dioxide. *Proceedings of the National Academy of Sciences* 109 (26), pp. 10164-10168.